Bioresource Technology 288 (2019) 121485

Contents lists available at ScienceDirect

Bioresource Technology

journal homepage: www.elsevier.com/locate/biortech

Pyrolysis kinetics of biomass wastes using isoconversional methods and the distributed activation energy model

Cindy Natalia Arenas[a], María Victoria Navarro[b], Juan Daniel Martínez[a,*]

[a] Grupo de Investigaciones Ambientales (GIA), Universidad Pontificia Bolivariana (UPB), Circular 1ra N° 74-50, Medellín, Colombia
[b] Instituto de Carboquímica (ICB-CSIC), Miguel Luesma Castán 4, 50018 Zaragoza, Spain

GRAPHICAL ABSTRACT

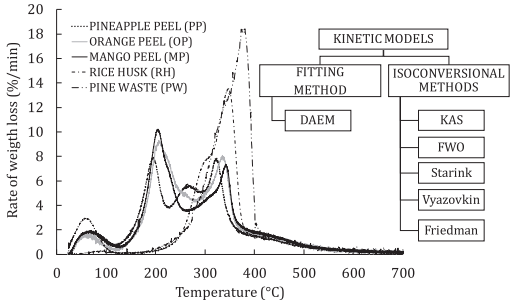

ARTICLE INFO

Keywords:
Biomass
Pyrolysis
Thermogravimetric analysis
Isoconversional methods
Kinetic models

ABSTRACT

In this work, a thermogravimetric analyser was used to assess the pyrolysis kinetics of pineapple, orange and mango peel wastes and agro-industrial by-products, rice husk and pine wood. Five isoconversional methods (KAS, FWO, Starink, Vyazovkin and Friedman) and one model-fitting method (DAEM) accurately fitted the experimental data at three heating rates (5, 10 and 20 °C/min) between 10% and 90% conversion. These methods agree with the trends shown by the activation energy (E_a) distribution calculated, with fluctuations between 150 and 550 kJ/mol. The fluctuations of E_a in the whole range of conversion, in addition to a higher number of relevant reactions obtained by DAEM for fruit peel samples compared to agro-industrial samples, are associated with a higher extractive content in the peels. Kinetic parameters fitted by DAEM were successfully verified at the highest heating rate studied.

1. Introduction

Energy consumption is increasing worldwide every year, while the sources of fossil fuels are either dwindling or remaining constant. Moreover, the need to reduce the use of fossil fuels owing to increased CO_2 emissions and to expand use of alternative fuels such those made from wastes (so-called second generation biofuels) has become common knowledge. Furthermore, biomass is the only renewable source able to produce electricity, heat, fuels and chemical products, making it a highly strategic resource with which to face the challenges of near future. Waste management systems in developing economies are still insufficient and in some cases cause environmental problems because waste tends to be unseparated and disposed of in open landfill sites. Biomass wastes, particularly those derived from food and agro-industry sector, are plentiful throughout the world, carbon–neutral, and can be regarded as a promising renewable energy resource.

* Corresponding author.
E-mail address: juand.martinez@upb.edu.co (J.D. Martínez).

https://doi.org/10.1016/j.biortech.2019.121485
Received 15 March 2019; Received in revised form 10 May 2019; Accepted 13 May 2019
Available online 15 May 2019

In Colombia, approximately 741,300 tonnes of pineapple (Procolombia, 2017), 238,100 tonnes of oranges (FAO, 2017), 318,628 tonnes of mango (Procolombia, 2017), and 2.1 million tonnes of rough (paddy) rice were produced in 2015 (FAO, 2016). In addition, there are approximately 330,000 ha of land planted with pine species (Pérez et al., 2017). Pineapple, orange and mango peels represent 29–40% (Ketnawa et al., 2012), 40–50% (Oberoi et al., 2010) and 15–20% (Ajila et al., 2007) of the gross weight of the fruit, respectively, while rice husk represents 20–23% of the gross weight of the grain (Martínez et al., 2011). Currently, both fruit peel wastes and agro-industrial by-products are managed as wastes, squandering their potential for use as feedstocks in other industrial processes such as in biorefineries.

Biomass and wastes can be transformed by thermochemical conversion processes such as pyrolysis, gasification and combustion. Besides being part of the first stages of the gasification and combustion processes, pyrolysis is gaining increasing attention given the possibility for producing a wide range of value-added products in the form of gases, liquids and solids, depending on the process conditions. Pyrolysis is generally an endothermic process performed in an oxygen-free atmosphere at temperatures of between 250 °C and 600 °C. In particular, the pyrolysis of lignocellulosic biomass involves many chemical and physical phenomena, resulting in a large number of intermediate and final products. Roughly speaking, there are three distinct steps in the pyrolysis process: i) drying, ii) primary reactions where volatile products are released and iii) secondary reactions where the primary products are subject to other reactions (Neves et al., 2011).

The kinetic analysis of any feedstock under pyrolysis conditions provides essential information on how it decomposes, allowing the optimization of the process and providing valuable information for reactor design. Kinetic analysis also reveals important data on the mechanism of reaction and establishes mathematical models that can describe the process (Huang et al., 2017). Kinetic studies on biomass pyrolysis are very frequent in the literature and they are addressed by two approaches: i) model-free (isoconversional) methods and ii) model-fitting methods (Vyazovkin and Wight, 1999; Vyazovkin et al., 2011; Mishra and Mohanty, 2018; He et al., 2019).

Isoconversional methods have the potential to estimate the behaviour of complex reactions; they are simple in nature; and they minimize the risks of selecting an unsuitable kinetic model and of finding the wrong kinetic parameters. Isoconversional methods have been widely used to examine the non-isothermal kinetic parameters of solid feedstocks in the pyrolysis processes (Huang et al., 2017; He et al., 2019), and they represent the most effective way with which to process thermogravimetric analysis (TGA) data in order to calculate effective activation energies for biomass pyrolysis (Cai et al., 2018). In addition, isoconversional methods constitute an interesting and easy-to-use solution for the estimation of kinetic parameters, providing rather accurate results in the case of a one-step reaction (Damartzis et al., 2011), with errors lower than 1% (Mishra and Mohanty, 2018). All isoconversional methods are based on the principle that the reaction rate at constant conversion degree is only a function of temperature (Vyazovkin et al., 2011). It is usually assumed that the activation energies for all reactions are depicted by a distribution of activation energies as a function of the conversion degree (Huang et al., 2017). If there is a substantial variation in activation energy over the extent of conversion, the kinetic parameters should be calculated by applying model-fitting methods with multi-step kinetic analysis in order to reproduce the reaction conversion (Vyazovkin et al., 2011).

With regards to model-fitting methods, the Distributed Activation Energy Model (DAEM) is an accurate, versatile and powerful tool for assessing the devolatilization kinetic process of different complex feedstocks such as coal (Pitt, 1962) or sewage sludge (Scott et al., 2006). DAEM has been previously pointed out by Varhegyi et al. (2002) as the best method available for mathematically representing the physical and chemical heterogeneity of biomass during a devolatilization process, and it has been successfully applied to woody biomass, including its major constituents (lignin, cellulose and hemicellulose) (Navarro et al., 2009), among others. DAEM is a multi-reaction model that assumes that the decomposition mechanism occurs through a large number of independent, parallel, first order or nth-order reactions with different activation energies reflecting variations in the bond strengths of species (Cai et al., 2014; Wang et al., 2017). The energy distribution of these reactions can be represented by a continuous function, such as Gaussian distribution, the Weibull distribution, the Fraser-Suzuki function and the logistic function (Wang et al., 2017), or also by a discrete distribution (Scott et al., 2006), which does not need a continuous function for the activation energy.

Isoconversional methods and DAEM have become an attractive alternative with which to perform a complete study of the pyrolysis kinetics of biomass derived from fruit peels. These methods have mainly been applied to conventional types of biomass and the literature is scarce as regards the feedstocks studied here. It is therefore of interest to assess how pyrolysis occurs and how comparable/reproducible the results of these methods will be when applied to different kinds of biomass. Literature shows works using isoconversional methods to determine the activation energy of different fruit peel wastes (Qiua et al., 2015; Sánchez et al., 2016; Tahir et al., 2019) and lignocellulosic by-products (Mishra and Mohanty, 2018; He et al., 2019) but there are no works, as the best authors' knowledge, using combined isoconversional methods and the DAEM approach given in this work to study and compare kinetics of fruit peels and lignocellulosic biomass.

2. Materials and methods

2.1. Feedstock

Five biomass wastes – pineapple peel (PP), orange peel (OP), mango peel (MP), rice husk (RH) and pine wood (PW) – were used in this work. Once collected, all samples were dried at 105 °C for 24 h in order to avoid the possible alteration of the main constituents. Elemental, proximate, heating value and extractive analyses were conducted on the five samples. Elemental analysis was performed using a Thermo Scientific Flash 2000 device. Proximate analysis was carried out according to the Spanish UNE-CEN/TS 14774-3 ex and UNE-CEN/TS14775 ex standards for determining moisture and ash content, respectively, while volatile matter was measured according to the oven-drying method specified by the ISO 5623:1974 standard. Fixed carbon was determined by difference. The higher heating value (HHV) was determined by applying the ASTM 240-09 standard using an IKA C2000 oxygen bomb calorimeter. Finally, extractives were quantified using the Tappi test method T 204 cm-17 for determining solvent extractives of wood and pulp.

2.2. Thermogravimetric analysis

TGA was performed under atmospheric pressure using a Q50 analyser (TA Instruments) at three different heating rates (5 °C, 10 °C and 20 °C/min). In all cases, the sample weight was fixed at 10 mg, while the particle size and the N_2 flow rate were 177–250 μm and 150 mL/min, respectively. The thermobalance was purged with N_2 for 10 min before starting the heating programme from room temperature to 700 °C. The temperature range for kinetic studies was taken as 110–700 °C as only moisture and physically absorbed water is removed at temperatures below 110 °C and there is negligible weight loss after 700 °C. The experimental conversion (X_{exp}) was calculated from Eq. (1).

$$X_{exp} = \frac{m_i - m}{m_i - m_f} \quad (1)$$

where m_i is the initial mass of sample (mg); m is the sample mass at time t (mg); and m_f is the sample mass (mg) at 700 °C.

Table 1
Isoconversional methods used in this work.

Method	Mathematical expression	Observations	Eq.	Ref.
KAS	$Ln\left(\frac{\beta_i}{T_{X,i}^2}\right) = C_{KAS} - \left(\frac{E_a}{RT_{X,i}}\right)$	Where β_i is the heating rate and C_{KAS} is a constant proper of the method	2	Kissinger (1956), Akahira and Sunose (1971)
FWO	$Ln(\beta_i) = C_{FWO} - 1.052\left(\frac{E_a}{RT_{X,i}}\right)$	Based on Doyle's approximation. C_{FWO} is a constant proper of the method	3	Flynn and Wall (1966), Ozawa (1965)
Starink	$Ln\left(\frac{\beta_i}{T_{X,i}^{1.92}}\right) = C_S - 1.0008\left(\frac{E_a}{RT_{X,i}}\right)$	Based on KAS and FWO methods. Cs is a constant proper of the method	4	Starink (1996)
Vyazovkin	$\Phi(E_a,X) = \sum_{i=1}^{\mu}\sum_{j\neq i}^{\mu}\frac{\beta_j I(E_a,T_{X,i})}{\beta_i I(E_a,T_{X,j})} = \mu(\mu-1)$	$I(E_a, T_{X,i})$ and $I(E_a, T_{X,j})$ represent the integral temperature $p(\lambda)$ corresponding to the heating rates β_i and β_j, respectively. The apparent E_a is given by the value that minimizes Φ. μ is number of experiments at different heating rates	5	Vyazovkin (1996), Vyazovkin et al. (2011), Rueda-Ordóñez and Tannous (2016)
	$I(E_a,T_X) = \int_0^{T_X} exp\left(\frac{-E_a,X}{RT}\right)dT = p(\lambda)$	Based on a non-linear technique, which uses a revised expression for the temperature integral ($p(\lambda)$). E_a is evaluated for a set of μ experiments conducted at different heating rates, β_i and β_j, where the subscripts i and j denote the ordinal number of the experiment.	6	
	$p(\lambda) = a\left(\frac{b}{c}\right)$ $a = \left(\frac{e^{-\lambda}}{\lambda}\right)$ $b = \lambda^7 + 70\lambda^6 + 1886\lambda^5 + 24920\lambda^4 + 170136\lambda^3 + 577584\lambda^2 + 844560\lambda + 357120$ $c = \lambda^8 + 72\lambda^7 + 2024\lambda^6 + 28560\lambda^5 + 216720\lambda^4 + 880320\lambda^3 + 1794240\lambda^2 + 1572480\lambda + 403200$	$I(E_a, T_X)$ can be determined by numerical integration or the Senum-Yang approximation	7	
Friedman	$Ln\left(\frac{dX}{dt}\right) = Ln\left[\beta_i\left(\frac{dX}{dT}\right)_{X,i}\right] = C_F - \frac{E_{a,X}}{RT_{X,i}}$	C_F is a constant proper of the method.	8	Friedman (1964)

2.3. Isoconversional methods

Five isoconversional methods were implemented in this work: (i) Kissinger-Akahira-Sunose (KAS), (ii) Flynn-Wall-Ozawa (FWO), (iii) Starink and (iv) Vyazovkin, all them in the integral form, while (v) the Friedman method was used in the differential form. Table 1 shows the mathematical expressions of these methods. These isoconversional methods enabled estimation of E_a at different conversion values, avoiding the uncertainty introduced by the reaction model assumption. Other kinetic parameters require knowledge of the reaction model. The conversion range used for obtaining the activation energy distribution was 10–90%, as recommended elsewhere (Vyazovkin et al., 2011).

2.4. Distributed activation energy model

DAEM describes the pyrolysis of complex feedstocks as many parallel decomposition reactions related to many different chemical groups. In this work, the algorithm developed by Scott et al. (2006) was implemented in a Fortran subroutine to solve this model. Thus, the unique triplet that characterizes each chemical group by its activation energy and pre-exponential factor of a first-order reaction was determined. This algorithm solves the kinetics of such reactions provided that only one reaction is dominating the overall loss of mass at the conversion of interest, as shown in Eq. (9).

$$X = \sum_i f_{i,0}\, exp\left[-A_i \int_0^t exp\left(-\frac{E_{a,i}}{RT(t)}\right)dt\right] \tag{9}$$

where X is the conversion degree; $f_{i,0}$ is the mass-fraction of m_i that decomposes with an activation energy $E_{a,i}$ (kJ/mol) and a pre-exponential factor A_i (s^{-1}); t is time (s); T is temperature (K); and R is the ideal gas constant (kJ/mol.K). Using experimental measurements of mass of sample at time t (m) at two different heating rates, the kinetic parameters of E_{ai}, A_i, $f_{i,0}$, were evaluated at 81 equally spaced intervals of conversion, corresponding to the conversion range of 10–90% with a step size of 1. The TGA data of heating rates of 5 °C and 10 °C/min were used in the model for determining the parameters then used to predict data at the heating rate of 20 °C/min.

2.5. Statistical treatment

The deviation in the determination of E_a for each sample using the KAS, FWO, Starink and Friedman methods was calculated from the regression coefficient (R^2). Likewise, the resulting deviation in the Vyazovkin method was performed by calculating a percentage error (*PE*) between the predicted values when Eq. (5) is minimized and the resulting value from μ(μ-1) (Vyazovkin, 1996).

On the other hand, application of DAEM enabled a simulated pattern to be obtained for the thermal degradation of each feedstock, which was validated by using the experimental TGA obtained at 20 °C/min. The deviation between the experimental and the simulated results from DAEM was assessed using mean absolute percentage error (*MAPE*), as expressed in Eq. (10). *MAPE* has been used to determine the goodness of fit of different structural models for biomass char gasification kinetics, as shown by Kramb et al. (2014).

$$MAPE(\%) = \frac{1}{g}\sum_{i=1}^{g}\left|\frac{X_{exp,i} - X_{theo,i}}{X_{exp,i}}\right| \times 100 \tag{10}$$

where g is the number of data points.

3. Results and discussion

3.1. Feedstock characterization

Table 2 shows the elemental, proximate, heating value and extractive analyses of the five biomass wastes considered in this work. As

Table 2
Elemental, proximate, extractives and heating value analyses.

Feedstock	Elemental analysis db (wt%)					Proximate analysis db (wt%)			Extractives db (wt%)	HHV db (MJ/kg)
	C	H	O	N	S	VM	A	FC		
PP	45.79	5.31	33.58	< 0.10	< 0.10	75.38	5.21	19.61	33.33	19.02
OP	46.04	5.54	36.89	0.65	< 0.10	79.02	3.43	17.54	34.53	18.57
MP	47.31	5.77	35.78	< 0.10	< 0.10	78.78	2.82	18.54	29.42	18.36
RH	41.13	3.37	38.17	0.33	< 0.10	71.28	17.01	11.72	10.56	15.30
PW	52.99	6.30	40.59	0.13	< 0.10	82.82	0.64	16.54	9.36	20.37

VM: Volatile Matter, A: Ash, FC: Fixed Carbon, C: Carbon, H: Hydrogen, O: Oxygen, N: Nitrogen; S: Sulphur, db: dry basis, HHV: Higher Heating Value.

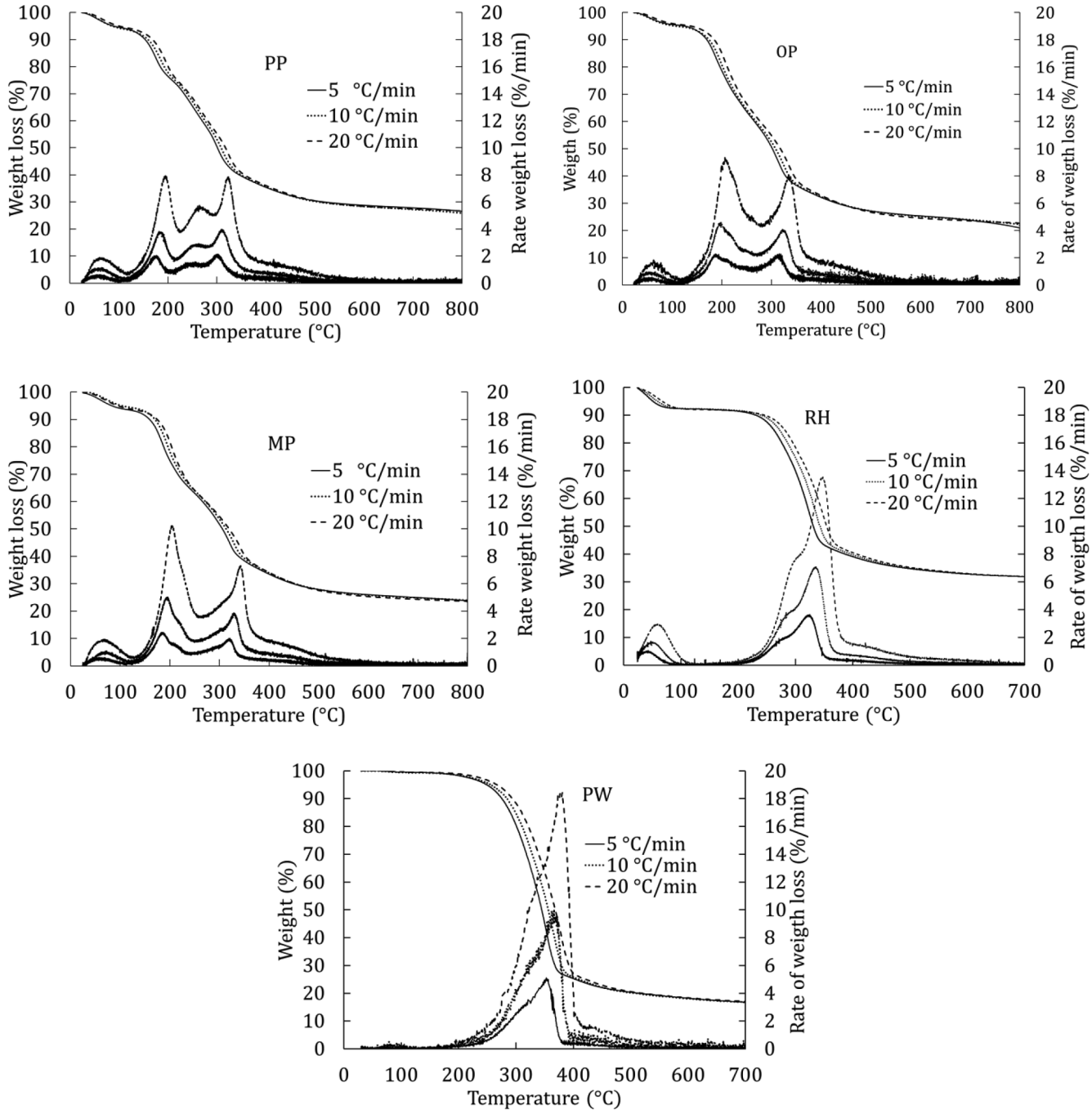

Fig. 1. Experimental TGA data.

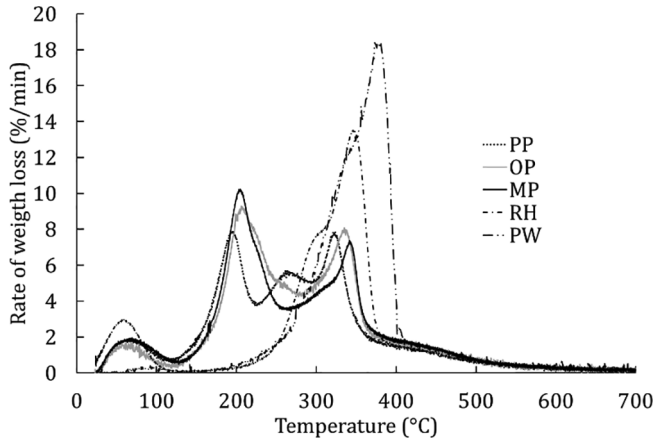

Fig. 2. Conversion rate comparison of samples at 20 °C/min.

expected, all samples show intermediate carbon content (41.13–49.70 wt%), while oxygen content is quite high (33.58–44.40 wt%). Hydrogen, nitrogen and sulphur content is relatively similar, with no major differences between them. In general terms, all these elements come from the main organic constituents of biomass such as cellulose, hemicellulose and lignin, as well as fractions of extractives (Sharma et al., 2015). Similarly, the volatile matter content for all samples is relatively high (75.38–82.82 wt%), enhancing their potential use as feedstock in pyrolysis processes for bio-oil production (Sait et al., 2012). Moreover, the ash content is very high for RH (17.01 wt%), while in the rest of samples it is relatively comparable (2.82–5.21 wt%), except for PW, which is very low (0.64 wt%). The HHV for the fruit peel wastes and agro-industrial by-products are between 18.36 and 19.02 MJ/kg, and 15.30 and 20.37 MJ/kg, respectively. On the other hand, the extractive contents vary notably between the fruit peel wastes and the agro-industrial by-products. The extractive contents of PP, OP and MP are 33.33 wt%, 34.53 wt% and 29.42 wt%, respectively; while their proportion in RH and PW is 9.36 wt% and 10.56 wt%, respectively.

3.2. Pyrolysis pattern

Fig. 1 shows the weight and the rate of weight loss for all samples at three different heating rates (5 °C, 10 °C and 20 °C/min). All fruit peel wastes show a relatively similar pattern. The first low peak is associated with the release of weakly bonded water. Then, two main peaks with maxima before 200 °C and after 300 °C remain almost equal for these three feedstocks, although intermediate shoulders or low peaks also appear between them, depending on the fruit peel waste. As they are biomass, they form a complex solid mainly composed of hemicellulose, cellulose, lignin (Wang et al., 2017) and inorganic compounds such as alkali metals (Sharma et al., 2015). These samples also present important fractions (around 30 wt% of composition, see Table 2) of extractives, (waxes, fats, resins, tannin, simple sugars, pectins and phenolic compounds, among others) that affect the decomposition profile since they show a wide decomposition range (150–600 °C).

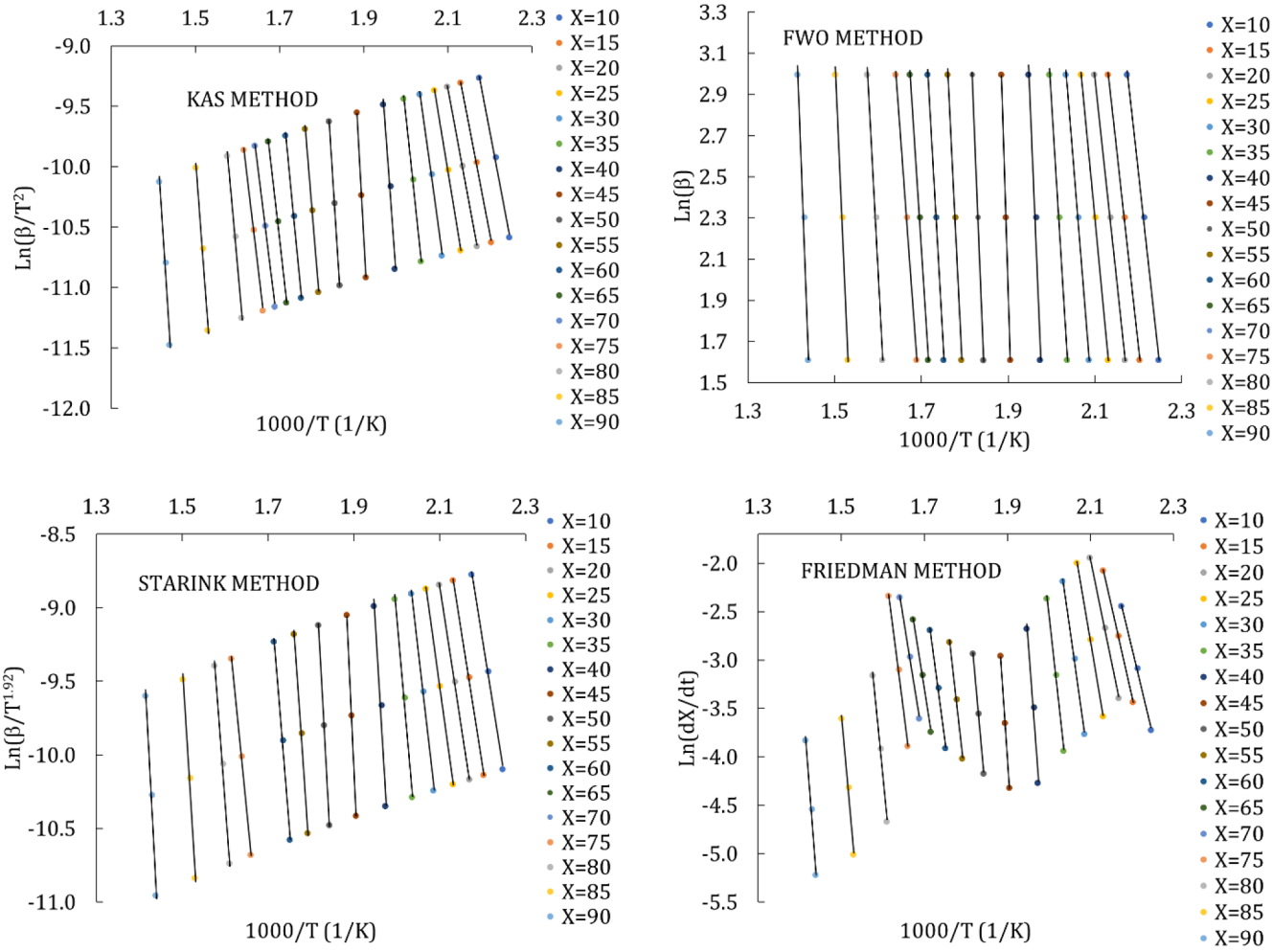

Fig. 3. Adjustment example of the isoconversional methods for MP.

Table 3
Deviation parameters in the adjustment of the isoconversional methods.

Feedstock	R^2								*PE* (%)	
	KAS		FWO		Starink		Friedman		Vyazovkin	
	Min	Max	Min	Max	Min	Max	Min	Max	Min	Max
PP	0.8314	0.9991	0.8406	0.9964	0.8318	0.9991	0.8287	1.0000	0.0380	7.8042
OP	0.8815	0.9960	0.8861	0.9964	0.8817	0.9960	0.8912	0.9962	0.1740	5.5461
MP	0.9641	1.0000	0.9656	1.0000	0.9642	1.0000	0.9690	0.9998	0.0005	1.6624
RH	0.9992	1.0000	0.9993	1.0000	0.9992	1.0000	0.9970	1.0000	0.0008	0.0351
PW	0.9981	1.0000	0.9982	1.0000	0.9981	1.0000	0.9984	1.0000	0.0006	0.0856

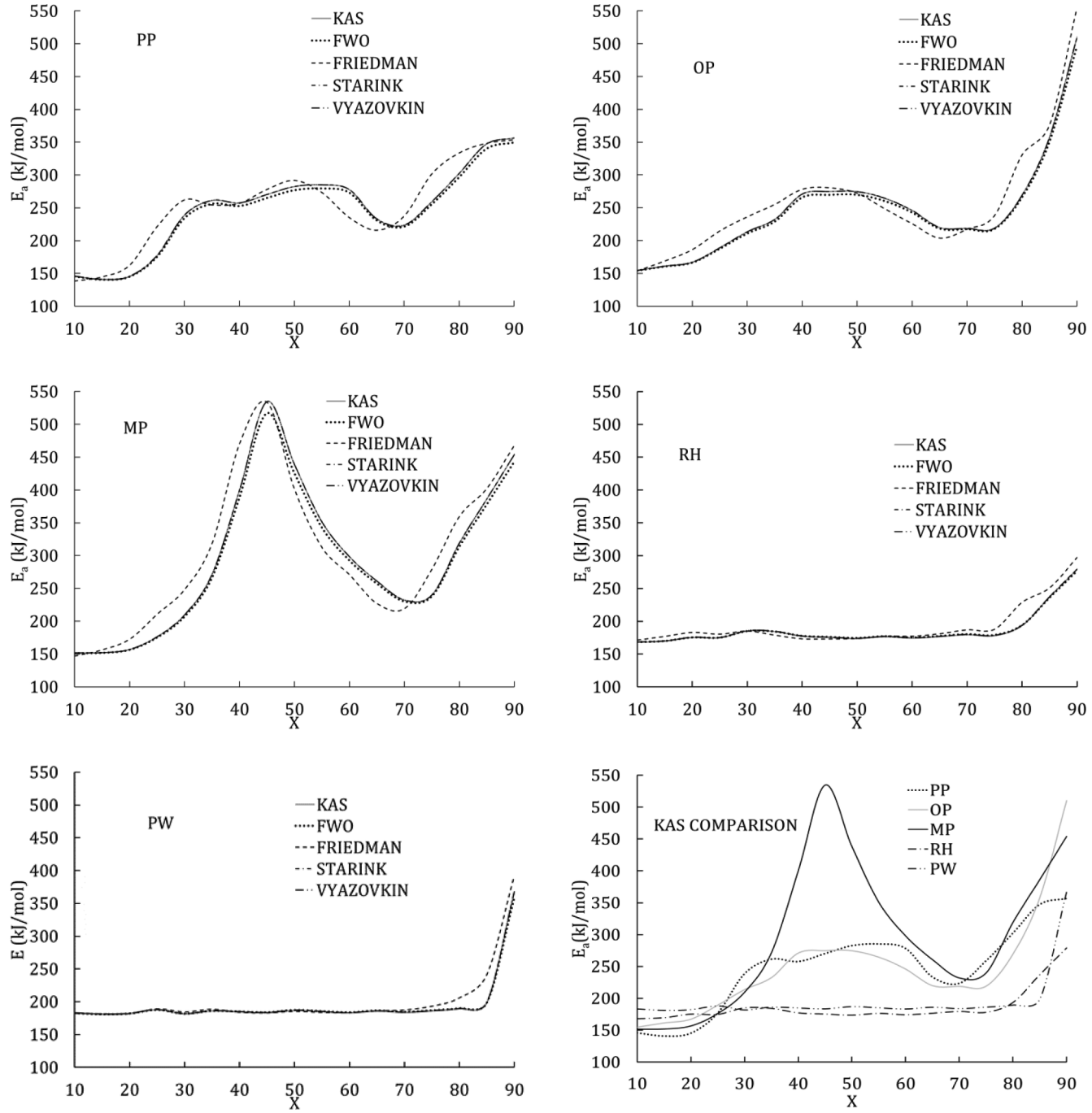

Fig. 4. E_a distribution from isoconversional methods.

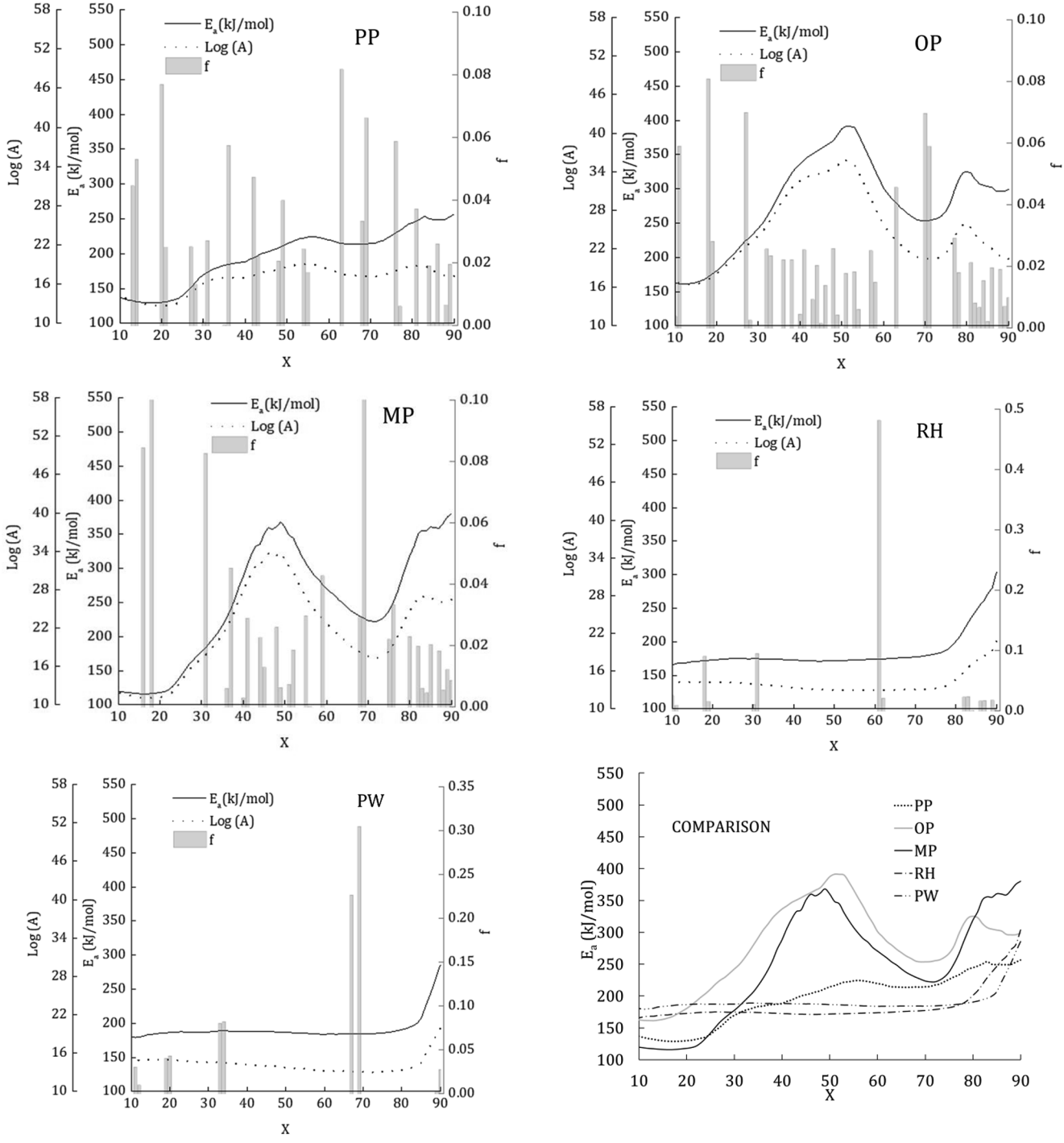

Fig. 5. Pyrolysis kinetic parameters obtained from DAEM.

As observed in Fig. 1, the degradation profile of these extractives overlaps with those from hemicellulose, cellulose and lignin (Guo et al., 2010; Özsin and Pütün, 2017). The decomposition pathway of the fruit peel wastes starts at around 150 °C with the hydrolysis of certain extractives (White et al., 2011), which are less stable and start to degrade at lower temperatures due to their higher volatility (Shebani et al., 2008; Părpăriţă et al., 2014). The decomposition of hemicellulose could be related to the secondary peak observed for PP and shoulders for OP and MP between 200 °C and 300 °C (Părpăriţă et al., 2014). The main fast devolatilization of the cellulose component between 300 °C and 350 °C produces the second main decomposition peak of the profiles (Părpăriţă et al., 2014). At higher temperatures, decomposition of the strongest bonds in the lignin takes place up to 550 °C (Özsin and Pütün, 2017; Brebu et al., 2014).

Finally, at the highest temperatures studied, only advanced charring processes continue with a very low reaction rate (Părpăriţă et al., 2014). The residual weight observed at 550 °C is about 28 wt% for these samples, while the final residual weight at 700 °C is about 25 wt%, indicating that the decomposition process is almost finished at 550 °C. Similar behaviour in the TGA pattern was also reported by Pathak et al. (2017) for different fruit peel wastes including banana, orange, citrus, lemon and jackfruit. Tahir et al. (2019) and Sánchez et al. (2016) also shown a very similar TGA profile for banana peels and pineapple peels, respectively. In addition, it is worth highlighting that the content and

Table 4
Fitting deviations for DAEM.

β (°C/min)	Feedstock	Conversion		Conversion rate	
		R^2	MAPE (%)	R^2	MAPE (%)
5	PP	1.0000	0.1207	0.9991	1.4368
	OP	1.0000	0.0852	0.9992	1.2464
	MP	1.0000	0.1110	0.9988	1.3162
	RH	1.0000	0.9039	0.9998	3.5692
	PW	1.0000	0.2277	0.9972	4.1965
10	PP	1.0000	0.3357	0.9986	1.6358
	OP	0.9999	0.5357	0.9948	2.5809
	MP	0.9999	1.9675	0.9864	3.3803
	RH	1.0000	1.1773	0.9993	5.9338
	PW	1.0000	0.3864	1.0000	3.1884
20	PP	0.9997	2.5675	0.9781	3.9015
	OP	0.9995	1.7507	0.9713	6.3223
	MP	0.9998	2.6367	0.9662	5.0798
	RH	1.0000	1.0691	1.0000	1.0691
	PW	0.9999	0.5066	0.9946	4.2809

character of extractives vary from type to type of biomass, even varying between different parts of each plant (Pecha and Garcia-Perez, 2015). With regard to RH and the PW, which have a much lower content in extractives (Table 2), thermal decomposition is mainly assigned to the degradation of cellulose, hemicellulose and lignin. In this case, all of them are superimposed onto a same shoulder peak between 250 °C and 400 °C. These results are similar to those reported by Zhang et al. (2016) for RH as well as those showed by Puy et al. (2011), Mishra and Mohanty (2018), and He et al. (2019) for PW.

Fig. 2 shows the comparison of the rate of weight loss for all samples at 20 °C/min. As observed, the maximum rate of weight loss for all the fruit peel wastes occurred close to 200 °C, while this temperature is higher for RH and PW, at around 350 °C and 380 °C, respectively. The different trends of rate weight loss for the fruit peel wastes and agro-industrial by-products are attributed to the composition, particularly cellulose, hemicellulose, lignin and extractive components. As shown in Table 2, the fruit peel wastes studied in this work showed higher extractives and hence, lower content in cellulose, hemicellulose and lignin than that found in lignocellulosic biomass, RH and PW, as reported elsewhere (Guo et al., 2010; Zhang et al., 2016; Mishra and Mohanty 2018).

3.3. Isoconversional methods

The E_a calculated for all the isoconversional methods considered in this work was obtained by linear regression. The plot of Ln (β/T^2) for the KAS method, the plot of Ln (β) for the FWO method, the plot of Ln ($\beta/T^{1.92}$) for the Starink method and the plot of Ln (β (dX/dT)) for the Friedman method, all them vs. 1000/T (K^{-1}), enabled to find the E_a using the TGA results for a conversion range between 10% and 90%, using a step size of 5. For example, Fig. 3 shows these adjustments for MP. Table 3 shows the minimum and maximum R^2 obtained for each feedstock and each isoconversional method (each model has 17 R^2 values for each sample). As observed, all the adjustments present a high R^2, greater than 0.8217. The Vyazovkin method is not shown in Fig. 3 because E_a was determined by minimization of Eq. (5). As previously mentioned, *PE* was used as a deviation indicator for this isoconversional method, resulting in values lower than 7.8042% (Table 3).

Fig. 4 shows E_a distribution against X of all feedstock for the KAS, FWO, Starink, Friedman and Vyazovkin methods and a comparison of them applying KAS method. As observed, E_a profiles are quite comparable for all isoconversional methods. In this sense, the E_a profiles of both fruit peel wastes and agro-industrial by-products for the KAS, FWO, Starink and Vyazovkin methods are practically the same. Since these methods are based on an integral form, there are some approximations associated with the temperature function (Jankovic, 2008; Mishra et al., 2015). However, the E_a profiles from the Friedman method are slightly different from those obtained using the other isoconversional methods. The Friedman method is based on the simple differential form of the kinetic rate law and involves no oversimplified approximation to assess the temperature function (Mishra et al., 2015). In addition, the Friedman method is not limited to the use of the linear variation of the heating rate (Cai et al., 2018).

In relation to the different E_a distributions obtained for the five samples, the fluctuations observed suggest the appearance of complex multi-step reactions including parallel, competitive and consecutive reactions (Vyazovkin et al., 2011). Different trends can be appreciated for each biomass type, as expected. In general terms, E_a changes notably as conversion increases for fruit peel wastes for the whole range of conversion studied, while it remains fairly stable for the agro-industrial by-products up to 80% conversion. The wide variation in E_a profiles are attributed to changes in the decomposition mechanism given the proportions of reactive compounds as well as the occurrence of possible secondary reactions such as cooking/charring (Chen et al., 2015).

PP shows an E_a profile tending to increase gradually with conversion (from 120 to 250 kJ/mol), with a brief and smooth decrease at $55\% > X > 75\%$. OP and the MP show a similar pattern. The E_a increases slowly with conversion and achieves a maximum around 400 kJ/mol for OP and 350 kJ/mol for MP when conversion is around 50%. After that, the E_a decreases slowly at conversions around 70% and 75% for OP and MP, respectively; and then increases again. Furthermore, the E_a profiles for RH and PW are stable within a wide conversion range ($10\% < X < 80\%$) with E_a around 170 kJ/mol for RH and 180 kJ/mol for PW. In both cases, E_a increases at high conversions (around 80%), reaching values around 300 kJ/mol for both feedstocks. The E_a found by Mishra and Mohanty (2018) was also around 170 kJ/mol for three waste sawdust biomasses obtained using different isoconversional methods (KAS, FOW, Friedman and Coats-Redfern) between 10% and 70% conversion. Similarly, He et al. (2019), reported an E_a profile around 170 kJ/mol (between 10% and 70% conversion) for the pyrolysis of PW. This value seems to increase after 70% conversion, especially when the Friedman method is used. The high E_a at conversion higher than 80%, obtained at temperatures higher than 350 °C, is related to the more difficult decomposition of the strongest bonds in the lignin content (Brebu et al., 2014; Özsin and Pütün, 2017) as well as possible cooking/charring reactions at higher conversions (Părpăriţă et al., 2014). In summary, although not at all conversion degrees, the fruit peel wastes showed the highest E_a values as compared to those of the agro-industrial by-products for most of the decomposition process. These results are in line with those values reported in literature by Sánchez et al. (2016) for fruit peels and by Mishra and Mohanty (2018) and He et al. (2019) for agro-industrial by-products.

3.4. Discrete distributed activation energy model

Unlike isoconversional methods, model-fitting methods as DAEM allows the prediction of the kinetic pyrolysis behaviour of complex feedstock such as those studied in this work. In this sense, Fig. 5 depicts the results of kinetic parameters (E_a, A and f) obtained from the model application to the TGA experiments at 5 and 10 °C/min for all feedstocks. In addition, a comparison of the E_a profiles obtained is introduced. As observed, the E_a profiles are consistent with the results obtained from the isoconversional methods (Fig. 4), particularly for the agro-industrial by-products. These profiles show notable changes in the E_a distribution with conversion for the fruit peel wastes and stable lower activation energies for the agro-industrial by-products. The E_a distributions obtained for the fruit peel wastes show the same fluctuating trend in the whole range on conversions as those calculated by isoconversional methods, although for the OP exhibited a wider and tallest peak between 20% and 70% conversion. These differences in the values obtained by model-free methods and DAEM suggest that the

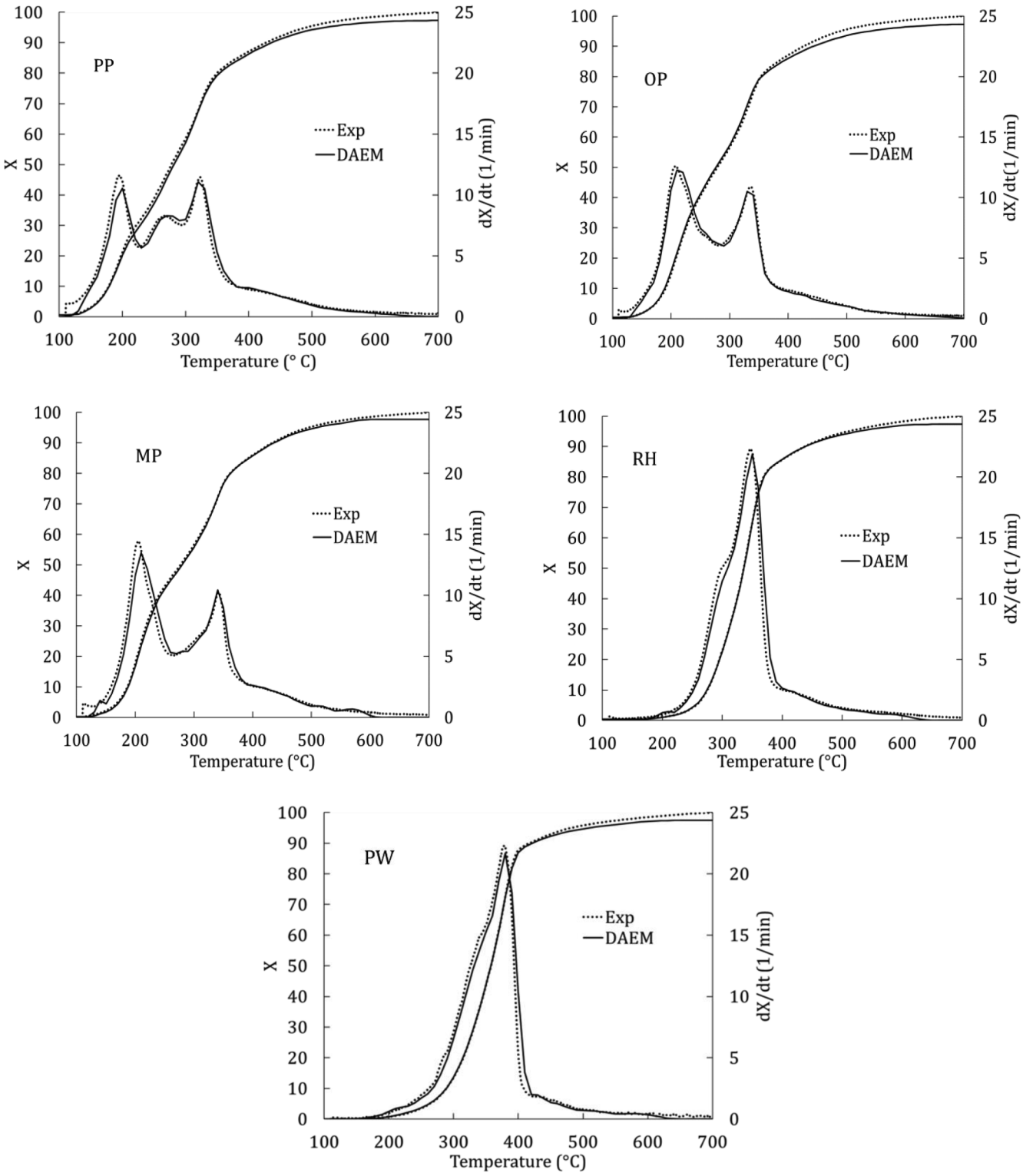

Fig. 6. Comparison between experimental data and theoretical data generated with DAEM algorithm at 20 °C/min.

higher complexity of the fruit peel samples affects E_a determination. On the other hand, E_a distributions calculated for the agro-industrial by-products are stable up to conversions of 80%. They perfectly reproduce the E_a distributions obtained with isoconversional methods. By DAEM application as well as by isoconversional methods, the fruit peel wastes showed the highest E_a values as compared to those of the agro-industrial by-products. These higher values indicate higher requirement of energy to process fruit peels completely that should be taken into account when designing pyrolysis systems.

Fig. 5 also shows the pre-exponential factor (A) and the resulting fraction of mass (f) associated with every reaction. The A profiles are very similar to those found for E_a, which is ascribed to the so-called energy compensation effect (Navarro et al., 2009; Vyazovkin et al., 2011; Chen et al., 2015). With regard to f_i, none of the reactions for PP, OP or MP have associated fractions higher than 0.10. Therefore, the pyrolysis process for fruit peel wastes seems to be characterized by 24

to 32 dominating reactions. Although hemicellulose, cellulose and lignin intervene, these reactions are mainly associated with the complex distribution and content of extractives in the fruit peel wastes. On the contrary, RH and PW show maximum mass fractions of 0.50 and 0.30, respectively. Fig. 5 also reveals that in both cases, more than 50% of the reactions take place through the reactions described at 60% and 69% of conversion, respectively, which have been assigned to conversion of cellulose component of the lignocellulosic biomass (Navarro et al., 2009). The pyrolysis of these two agro-industrial by-products seems to be described by 8 to 12 dominating reactions, mainly associated with hemicellulose, cellulose and lignin degradation (Navarro et al., 2009; Zhou et al., 2018). Both the fluctuations of E_a throughout the entire conversion range and the higher number of relevant reactions obtained by DAEM for the fruit peel wastes, as compared to the agro-industrial by-products, described more heterogeneous and complex samples associated with a higher extractive content in the former.

3.5. Kinetic model validation

The E_a, A and f determined by DAEM also enabled modelling of the pyrolysis behaviour of all five feedstocks at the three heating rates studied in this work. All the experimental kinetic curves were satisfactorily reproduced with deviations between experimental and predicted data using R^2 and *MAPE* for both the conversion and the conversion rate compiled in Table 4. In all cases, R^2 values are very close to 1, while the maximum *MAPE* is less than 2.7% and 6.4% for conversion and conversion rate, respectively.

Fig. 6 shows the validation of kinetic parameters obtained by DAEM for the TGA experiments conducted at 20 °C/min. Data from this heating rate were not included in the kinetic computations using the DAEM approach and hence, a more rigorous validation test was ensured, as suggested by Vyazovkin et al. (2011). As observed, the model perfectly simulated the temperatures required to achieve a conversion up to 90% for all the feedstocks studied. Despite some slight differences at conversions higher than 95%, it should be highlighted that DAEM results for all samples (fruit peel wastes and agro-industrial by-products) at this higher heating rate show remarkably good agreement with the experimental data. More particularly, the model accurately reproduces the shape of conversion and reaction rate profiles with the shift to higher temperatures related to the increasing heating rate, given that the experimental and calculated profiles overlap. These results indicate the great accuracy of DAEM for predicting pyrolysis kinetics of biomass wastes of different characteristics.

4. Conclusions

The E_a distribution for fruit peel wastes showed a fluctuating profile throughout the entire range of conversion (150–550 kJ/mol), while it showed a stable profile (180 kJ/mol) for the agro-industrial by-products up to 80% conversion. The six methods used to determine E_a showed similar patterns. The resulting fraction of mass distributions obtained by DAEM for fruit peel wastes and agro-industrial by-products are characterized by 24 to 32 and by 8 to 12 relevant reactions, respectively. Both the fluctuating E_a and high number of relevant reactions are associated with a high extractive content in the peel samples ($\approx$30 wt %).

Acknowledgements

The authors would like to express all their gratitude to COLCIENCIAS and CIDI-UPB for the financial support given by the projects 1210-715-51742 and 387C-11/18-24, respectively. We are also grateful to GIMEL group from UdeA for making the TGA device available to us, and to the GRAIN group from UPB for their support in extractives quantification. In addition, the authors would like to thank MINECO and FEDER for their financial support (Project ENE2015-68320-R) and the Regional Government of Aragon (DGA) for the support provided under their research groups support programme.

References

Ajila, C.M., Bhat, S.G., Prasada, U.J.S., 2007. Valuable components of raw and ripe peels from two India mango varieties. Food Chem. 102, 1006–1011.
Akahira, T., Sunose, T., 1971. Joint convention of four electrical institutes. Sci. Technol. 16, 22–31.
Brebu, M., Yanik, J., Uysal, T., Vasile, C., 2014. Thermal and catalytic degradation of grape seeds/polyethylene waste mixture. Cellul. Chem. Technol. 48, 665–674.
Cai, J., Wu, W., Liu, R., 2014. An overview of distributed activation energy model and its application in the pyrolysis of lignocellulosic biomass. Renew. Sust. Energy Rev. 36, 236–246.
Cai, J., Xu, D., Dong, Z., Yu, X., Yang, Y., Banks, S.W., Bridgwater, A.V., 2018. Processing thermogravimetric analysis data for isoconversional kinetic analysis of lignocellulosic biomass pyrolysis: case study of corn stalk. Renew. Sust. Energy Rev. 82, 2705–2715.
Chen, Z., Zhu, Q., Wang, X., Xiao, B., Liu, S., 2015. Pyrolysis behaviors and kinetic studies on Eucalyptus residues using thermogravimetric analysis. Energ. Convers. Manage. 105, 251–259.
Damartzis, Th., Vamvuka, D., Sfakiotakis, S., Zabaniotou, A., 2011. Thermal degradation studies and kinetic modeling of cardoon (Cynara cardunculus) pyrolysis using thermogravimetric analysis (TGA). Bioresour. Technol. 102, 6230–6238.
FAO, 2016. Rice market monitor. http://www.fao.org/fileadmin/templates/est/COMM_MARKETS_MONITORING/Rice/Images/RMM/RMM_APR16.pdf. (Access on 12.12. 2018).
FAO, 2017. Citrus fruit fresh and processed. http://www.fao.org/3/a-i8092e.pdf. (Access on 12.12.2018).
Friedman, H.L., 1964. Kinetics of thermal degradation of char-forming platics from thermogravimetry. Application to a phenolic plastic. J. Polym. Sci Part C: Polym. Sym. 6, 183–195.
Flynn, J.H., Wall, L.A., 1966. A quick, direct method for the determination of activation energy from thermogravimetric data. J. Polym. Sci Part B: Polym. Lett. 4, 323–328.
Guo, X.J., Wang, S.R., Wang, K.G., Liu, Q., Luo, Z.Y., 2010. Influence of extractives on mechanism of biomass pyrolysis. J. Fuel Chem. Technol. 38, 42–46.
Huang, Y.W., Chen, M.Q., Li, Y., 2017. An innovative evaluation method for kinetic parameters in distributed activation energy model and its application in thermochemical process of solid fuels. Thermochim. Acta 655, 42–51.
He, Q., Ding, L., Gong, Y., Li, W., Wei, J., Yu, G., 2019. Effect of torrefaction on pinewood pyrolysis kinetics and thermal behavior using thermogravimetric analysis. Bioresour. Technol. 208, 104–111.
Jankovic, B., 2008. Kinetic analysis of the nonisothemal decomposition of potassium metabisulfite using the model-fitting and isconversional (model-free) methods. Chem. Eng. J. 139, 128–135.
Ketnawa, S., Chaiwut, P., Rawdkuen, S., 2012. Pineapple waste: a potential source for bromelain extraction. Food Bioprod. Process. 90, 385–391.
Kramb, J., Konttinen, J., Gómez-Barea, A., Moilanen, A., Umeki, K., 2014. Modeling biomass char gasification kinetics for improving prediction of carbon conversion in a fluidized bed gasifier. Fuel 132, 107–115.
Kissinger, H.E., 1956. Variation of peak temperature with heating rate in differential thermal analysis. J. Res. Natl. Bur. Stand. 57, 217–221.
Martínez, J.D., Pineda, T., López, J.P., Betancur, M., 2011. Assessment of the rice husk lean-combustion in a bubbling fluidized bed for the production of amorphous silica-rich ash. Energy 36, 3846–3854.
Mishra, G., Kumar, J., Bhaskar, T., 2015. Kinetic studies on the pyrolysis of pinewood. Bioresour. Technol. 182, 282–288.
Mishra, R., Mohanty, K., 2018. Pyrolysis kinetics and thermal behaviour of waste sawdust biomass using thermogravimetric analysis. Bioresour. Technol. 251, 63–74.
Navarro, M.V., Murillo, R., Mastral, A.M., Puy, N., Bartoli, J., 2009. Application of the distributed activation energy model to biomass and biomass constituents devolatilization. AIChE J. 55, 2700–2715.
Neves, D., Thunman, H., Matos, A., Tarelho, L., Gómez-Barea, A., 2011. Characterization and prediction of biomass pyrolysis products. Prog. Energy Combust. Sci. 37, 611–630.
Oberoi, H.S., Vadlani, P.V., Madi, R.L., Saida, L., Abeykoon, J.P., 2010. Ethanol production from Orange peels: two-stage hydrolysis and fermentation studies using optimized parameters through experimental design. J. Agric. Food Chem. 58, 3422–3429.
Ozawa, T., 1965. A new method of analyzing thermogravimetric data. Bull. Chem. Soc. Jpn. 38, 1881–1886.
Özsin, G., Pütün, A.E., 2017. Kinetics and evolved gas analysis for pyrolysis of food processing wastes using TGA/MS/FT-IR. Waste Manage. 64, 315–326.
Părpăriţă, E., Brebu, M., Azhar, Md., Yanik, J., Vasile, C., 2014. Pyrolysis behaviors of various biomasses. Polym. Degrad. Stab. 100, 1–9.
Pathak, P.D., Mandavgane, S.A., Kulkarni, B.D., 2017. Fruit peel waste: characterization and its potential uses. Curr. Sci. 113, 444–454.
Pecha, B., Garcia-Perez, M., 2015. Pyrolysis of lignocellulosic biomass: oil, char, and gas. In: Dahiya, A. (Ed.), Bioenergy Biomass to Biofuels. Academic Press, pp. 413–442.
Pérez, J.F., Pelaez-Samaniego, M.R., Garcia-Perez, M., 2017. Torrefaction of fast-growing Colombian Wood species. Waste Biomass Valori. 1–13.
Pitt, G., 1962. The kinetics of the evolution of volatile products from coal. Fuel 41, 267–274.
Procolombia, 2017. Colombia an export and investment platform in the Americas. http://www.portmanatee.com/wp-content/uploads/2017/06/PPT_April-20-2017.pdf.

(Access on 12.12.2018).
Puy, N., Murillo, R., Navarro, M.V., López, J.M., Rieradevall, J., Fowler, G., Aranguren, I., García, T., Bartrolí, J., Mastral, A.M., 2011. Valorisation of forestry waste by pyrolysis in an auger reactor. Waste Manage. 31, 1339–1349.
Qiua, H.-W., Zhou, Q.-C., Geng, J., 2015. Pyrolytic and kinetic characteristics of Platycodon Grandiflorum peel and its cellulose extract. Carbohyd. Polym. 117, 644–649.
Rueda-Ordóñez, Y.J., Tannous, K., 2016. Thermal decomposition of sugarcane straw, kinetics and heat of reaction in synthetic air. Bioresour. Technol. 211, 231–239.
Sait, H.H., Hussain, A., Adam, A., Nasir, F., 2012. Pyrolysis and combustion kinetics of date palm biomass using thermogravimetric analysis. Bioresour. Technol. 118, 382–389.
Sánchez, J.D., Ramírez, G.E., Barajas, M.J., 2016. Comparative kinetic study of the pyrolysis of mandarin and pine apple peel. J. Anal. Appl. Pyrol. 118, 192–201.
Scott, S.A., Dennis, J.S., Davidson, J.F., Hayhurst, A.N., 2006. An algorithm for determining the kinetic of devolatilisation of complex solid fuel from thermogravimetric experiments. Chem. Eng. Sci. 61, 2339–2348.
Sharma, A., Pareek, V., Zhang, D., 2015. Biomass pyrolysis—A review of modelling, process parameters and catalytic studies. Renew. Sustain. Energy Rev. 50, 1081–1096.
Shebani, A.N., van Reenen, A.J., Meincken, M., 2008. The effect of wood extractives on the thermal stability of different wood species. Thermochim. Acta 471, 43–50.
Starink, M.J., 1996. A new method for the derivation of activation energies from experiments performed ar constant herating rate. Thermochim. Acta 288, 97–104.
Tahir, M.H., Zhao, Z., Ren, J., Rasool, T., Naqvi, S.R., 2019. Thermo-kinetics and gaseous product analysis of banana peel pyrolysis for its bioenergy potential. Biomass Bioenergy 122, 193–201.
Varhegyi, G., Szabó, P., Antal, M.J., 2002. Kinetics of charcoal devolatilization. Energ. Fuel 16, 724–731.
Vyazovkin, S., 1996. A unified approach to minetic processing of nonisothermal data. Int. J. Chem. Kinet. 28, 94–101.
Vyazovkin, S., Wight, C.A., 1999. Model-free and model-fitting approaches to kinetic analysis of isothermal and noisothermal data. J. Chem. Inf. Comput. Sci. 340–341, 53–68.
Vyazovkin, S., Burnham, A.K., Criado, J.M., Pérez-Maqueda, L.A., Popescu, C., Sbirrazzuoli, N., 2011. ICTAC Kinetics Committee recommendations for performing kinetic computations on thermal analysis data. Thermochim. Acta 520, 1–19.
Wang, S., Dai, G., Yang, H., Luo, Z., 2017. Lignocellulosic biomass pyrolysis mechanism: A state-of-the-art review. Prog. Energy Combust. Sci. 62, 33–86.
White, J.E., Catallo, W.J., Legendre, B.L., 2011. Biomas spyrolysis kinetics: a comparative critical review with relevant agricultura residual case studies. J. Anal. Appl. Pyrol. 91, 1–33.
Zhang, S., Dong, Q., Zhang, L., Xion, Y., 2016. Effects of water washing and torrefaction on the pyrolysis behavior and kinetics of rice husk through TGA and Py-GC/MS. Bioresour. Technol. 199, 352–361.
Zhou, B., Zhou, J., Zhang, Q., 2018. Research on pyrolysis of *Camellia sinesis* branches via the discrete distributed activation energy model. Bioresour. Technol. 241, 113–119.